UDK 616.288:612.063
Original scientific article/Izvirni znanstveni članek

ISSN 1580-2949
Mater. Tehnol.

MONITORING AND EVALUATION OF ERECTILE FUNCTION DURING ROBOT-ASSISTED RADICAL PROSTATECTOMY

SPREMLJANJE IN OCENJEVANJE EREKTILNE FUNKCIJE MED ROBOTSKO ASISTIRANO RADIKALNO PROSTATEKTOMIJO

Janez Rozman[1], Jure Bizjak[2], Matjaž Godec[3], Samo Ribarič[4], Simon Hawlina[2,5]*

[1]Center for Implantable Technology and Sensors, ITIS d. o. o. Ljubljana, Lepi pot 11, 1000 Ljubljana, Republic of Slovenia
[2]University Medical Centre Ljubljana, Department of Urology, Zaloška 2, 1000 Ljubljana, Republic of Slovenia
[3]Institute of Metals and Technology, Lepi pot 11, 1000 Ljubljana, Republic of Slovenia
[4]Institute of Pathophysiology, Faculty of Medicine, University of Ljubljana, Zaloška 4, 1000 Ljubljana, Republic of Slovenia
[5]Chair of Surgery, Faculty of Medicine, University of Ljubljana, Vrazov trg 2, 1000 Ljubljana, Republic of Slovenia

Prejem rokopisa – received: 2025-05-21; sprejem za objavo – accepted for publication: 2025-10-17

doi:10.17222/mit.2025.1461

To optimize the removal of cancerous prostate tissue, nerve-sparing robot-assisted radical prostatectomy (RARP) is commonly used. This technique aims to preserve the neurovascular bundles (NVBs), damage to which is a major cause of postoperative erectile dysfunction (ED). The primary goal of this study was to develop and assess a novel intraoperative NVB stimulation (NVBS) system designed to elicit penile erectile responses during RARP and assist in predicting postoperative erectile function (EF). The stimulation paradigm involved applying trains of rectangular and quasi-trapezoidal stimulating pulses (stimuli) to the apical, mid, and basal portions of the NVBs for approximately 60 s, both before and after the nerve-sparing dissection. The stimulation probe was developed with a consideration of nerve-stimulation models, NVB anatomy, and surgical constraints. Electrodes made of platinum were embedded in denture-grade material and mounted in a titanium housing. To evaluate the erectile responses, a multi-sensor probe was designed to monitor axial penile rigidity (ARIG), galvanic skin response (GSR), and glans temperature T_{gp}. Additionally, corpus cavernosum electromyography (CC-EMG) was recorded using surface and needle electrodes. Among five male patients enrolled, two showed noticeable CC-EMG activity, but none demonstrated a measurable increase in axial penile rigidity. The CC-EMG data were limited to short-term monitoring and could not be reliably analyzed in the time or frequency domains. In conclusion, although the stimulation protocol did not trigger measurable erectile responses, CC-EMG signals offered intraoperative insights into NVB integrity. This information may support more accurate predictions of erectile function recovery following RARP.

Keywords: robot-assisted radical prostatectomy, neurovascular bundles, electrical nerve stimulation, physiological measurements

Za optimalno odstranitev rakavega tkiva prostate se pogosto uporablja robotsko asistirana radikalna prostatektomija (RARP) z ohranjanjem živcev. Ta tehnika si prizadeva ohraniti nevrovaskularne snope (NVB), katerih poškodba je eden glavnih vzrokov za pooperativno erektilno disfunkcijo (ED). Glavni cilj te študije je bil razviti in oceniti nov sistem za intraoperativno stimulacijo NVB, zasnovan za izzivanje erektilnega odziva med RARP in pomoč pri napovedovanju pooperativne erektilne funkcije (EF). Stimulacijski protokol je vključeval uporabo pravokotnih in kvazi-trapeznih električnih impulzov, ki so bili aplicirani na apikalni, srednji in bazalni del NVB približno 60 sekund, pred in po disekciji z ohranjanjem živcev. Stimulacijska sonda je bila zasnovana z namenom zadostiti modelom živčne stimulacije, anatomiji NVB in kirurškim omejitvam. Elektrode iz platine so bile vgrajene v material za zobne proteze in pritrjene v titanovo ohišje. Za oceno erektilnega odziva je bila izdelana multisenzorična sonda, ki je merila aksialno togost penisa (ARIG), galvanski kožni odziv (GSR) in temperaturo glansa (T_{gp}). Sočasno je bila z uporabo površinskih in igelnih elektrod izvedena tudi elektromiografija korpusa kavernozuma (CC-EMG). Med petimi vključenimi bolniki sta dva pokazala zaznavno CC-EMG aktivnost, vendar noben ni izkazal merljivega povečanja aksialne togosti penisa. CC-EMG podatki so bili omejeni na kratkotrajno spremljanje in jih ni bilo mogoče zanesljivo analizirati v časovni ali frekvenčni domeni. Čeprav stimulacija ni sprožila merljivega erektilnega odziva, so CC-EMG signali nudili dragocene intraoperativne informacije o integriteti NVB. Te informacije lahko prispevajo k natančnejši napovedi okrevanja erektilne funkcije po RARP.

Ključne besede: robotsko asistirana radikalna prostatektomija, živčno žilni snopi, električna stimulacija živca, fiziološka merjenja

1 INTRODUCTION

Robot-assisted radical prostatectomy (RARP) is a widely used minimally invasive surgical technique for the treatment of clinically localized prostate cancer. Compared to open surgery, RARP offers advantages such as reduced blood loss, smaller incisions, less postoperative pain, and shorter hospital stays. Importantly, it facilitates nerve-sparing approaches, enhancing the possibility of preserving erectile function (EF) by minimizing trauma to neurovascular bundles (NVBs).

Despite advances in nerve-sparing techniques, postoperative ED remains a common complication. This is primarily due to mechanical and thermal damage to the NVBs during dissection.[1] Preservation of these structures is essential for EF recovery, yet predicting functional outcomes intraoperatively remains challenging.

*Corresponding author's e-mail:
simon.hawlina@kclj.si (Simon Hawlina)

Historical studies, beginning with Walsh et al. (1983), have laid the foundation for nerve-sparing radical prostatectomy by mapping pelvic-nerve anatomy.[2] Since then, anatomical studies and intraoperative stimulation trials have aimed to improve our understanding of NVB topography and develop strategies to preserve EF.[3–12]

However, the anatomical complexity and variability of NVBs continue to limit standardized approaches. The cavernous nerves (CNs) are the major autonomic nerves that innervate the penis. They mediate the relaxation/contraction of the Corpus Cavernosum muscle (CCM) and are responsible for the EF of penile tissue. They are very susceptible to injury that can occur during radical prostatectomy (RP). NVBs are tubular structures that bind interweaving autonomic fibers that innervate the CC and blood vessels within the connective tissue. They run posterolaterally between the lateral pelvic fascia and prostatic fascia along the surface of each side of the prostate and give off branches to the prostate at the apex and base.[13] The nerve branches within the the NVBs are thin and wiry similar to a strand of hair. They are extremily susceptible to stretch during RP. If the cancer tissue during the RP is not spread outside the prostate, the surgeon could accomplish a sparing of the nerves. NVBs could be separeted carefully away from the prostate and stay undamaged. It is one of the most delicate steps of the RP. The level of trauma applied to the NVBs that cannot be avoided during the nerve sparing determines the time needed for the nerve to recover its conduction to control EF. Recent efforts have explored intraoperative CN stimulation to assess NVB integrity.[14–17]

The goal of this study was to design and evaluate a novel intraoperative NVBS and monitoring system during RARP. Specifically, we aimed to determine the effectiveness of two types of stimuli in eliciting erectile responses and to monitor changes in ARIG, CC-EMG, GSR, T_{gp}. The ultimate aim was to contribute to more accurate and reliable intraoperative NVB mapping and predict functional outcomes following RARP.

2 EXPERIMENTAL PART

The experimantal protocol complied with the Declaration of Helsinki: recommendations guiding physicians in biomedical research involving human subjects. The study was approved by the National Medical Ethics Committee, Ministry of Health, Republic of Slovenia (Unique Identifier No. 0120-138/2024-2711-6).

Five subjects with clinically localized prostate cancer (stage T1 or T2) were enrolled in the study (mean age 57 years). They had a satissfactory preoperative EF (>23/25) according to the international index of erectile function (IIEF)). All were scheduled to undergo bilateral nerve-sparing surgery using RARP. The informed consent was signed after they were informed about the purpose and the procedures of the study. All subjects consented were registered in the University Medical Centre Ljubljana database. Taken safety precausions: the battery-powered experimental setup was out of galvanic

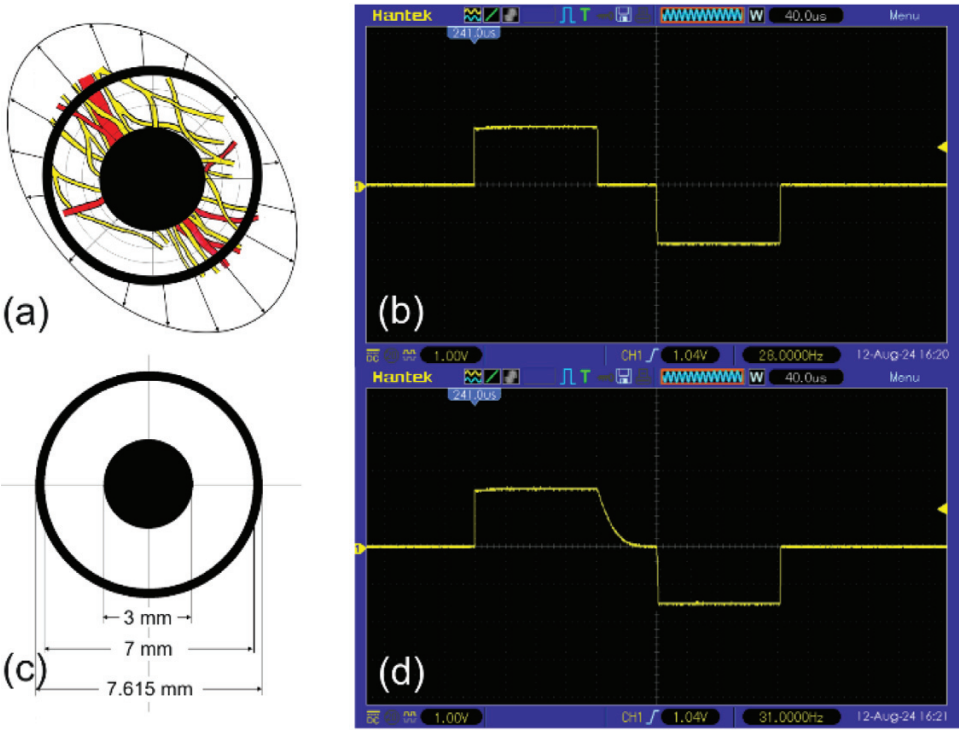

Figure 1: Schematic diagram of selective NVBS: a) stimulating cathode and anode above the NVB and scaled action potential propagation directions, b) waveform of rectangular stimulus, c) arrangement, shape and dimensions of stimulating electrodes, d) waveform of quasi-trapezoidal stimulus

contact with power lines, and cauter was not used at any moment during the experiment.

In this study, a paradigm of selective NVBS, shown in the **Figure 1**, was developed. **Figure 1a** shows stimulating electrodes above the NVB and action potential propagation directions. A paradigm proposed stimulation using two different current, biphasic, and charge-balanced stimuli. The first one, (**Figure 1b**), was composed of a rectangular cathodic intensity i_c and width t_c, followed by a delay d, and anodic intensity i_a and width t_a. **Figure 1c** shows the arrangement, shape and dimensions of the stimulating electrodes.

The second stimulus (**Figure 1d**) was an asymmetric stimulus, composed of a quasi-trapezoidal cathodic phase with a square cathodic intensity i_c, a plateau with the width t_c, followed by an exponentially decaying phase with the width t_{exp} and time constant τ_{exp}, and a rectangular anodic intensity i_a and width t_a.

Nerve fibers were depolarized below the cathode from where action potentials propagate via towards to the CCs.

2.1 Stimulating set-up

A stimulating probe (probe) was designed after considering literature on the modelling of peripheral nerve stimulation,[18] structural topography of the NVBs and physical limitations.

A material for stimulating electrodes was chosen based on mechanical and electrochemical characteristics.[19] With this regard, a 0.2-mm-thick cold-rolled platinum ribbon (purity 99.99 *w*/%) was used for the stimulating cathode while 0.31-mm-thick platinum ribbon was used for the anode. Crafting the cathode comprised cutting the 5.5-mm disc from the platinum ribbon, forging the disc into the 0.4-mm-high hat with a 3-mm diameter flat area and geometric surface of around 7 mm^2 and finally, welding the lead wires onto the hat bottom using a capacitive discharge spot welder.

Crafting the anode comprised cutting a 22-mm-long and 1.5-mm-wide strip from the platinum ribbon and bending it into a 1.5-mm-high ring with a 7-mm inner diameter. The geometric surface of the top edge of the ring-shaped anode was around 7 mm^2. The third step was welding the lead wires onto the bottom edge of the ring-shaped anode.

Leads to the electrodes were made using fluorinated ethylene propylene (FEP) insulated stainless-steel wire (AS 637, Cooner Wire, Chatsworth, CA).

The electrode arrangement was encapsulated using self-curing denture material (ProBase Cold Professional PMMA denture base material, Ivoclar, Schaan, Liechtenstein). An arrangement was inserted into the model made of silicone (Extreme Silicone) and filled with denture material. After the material cured, the casting was removed from the model and adhered into the titanium body using medical grade silicone adhesive (40064, MED RTV adhesive, Applied Silicone Corporation, Santa Paula, U.S.A.).

To generate stimuli, customized stimulator and voltage booster amplifier shown in **Figure 2a**, were used. **Figure 2b** shows the probe with central cathode and circumferential anode.

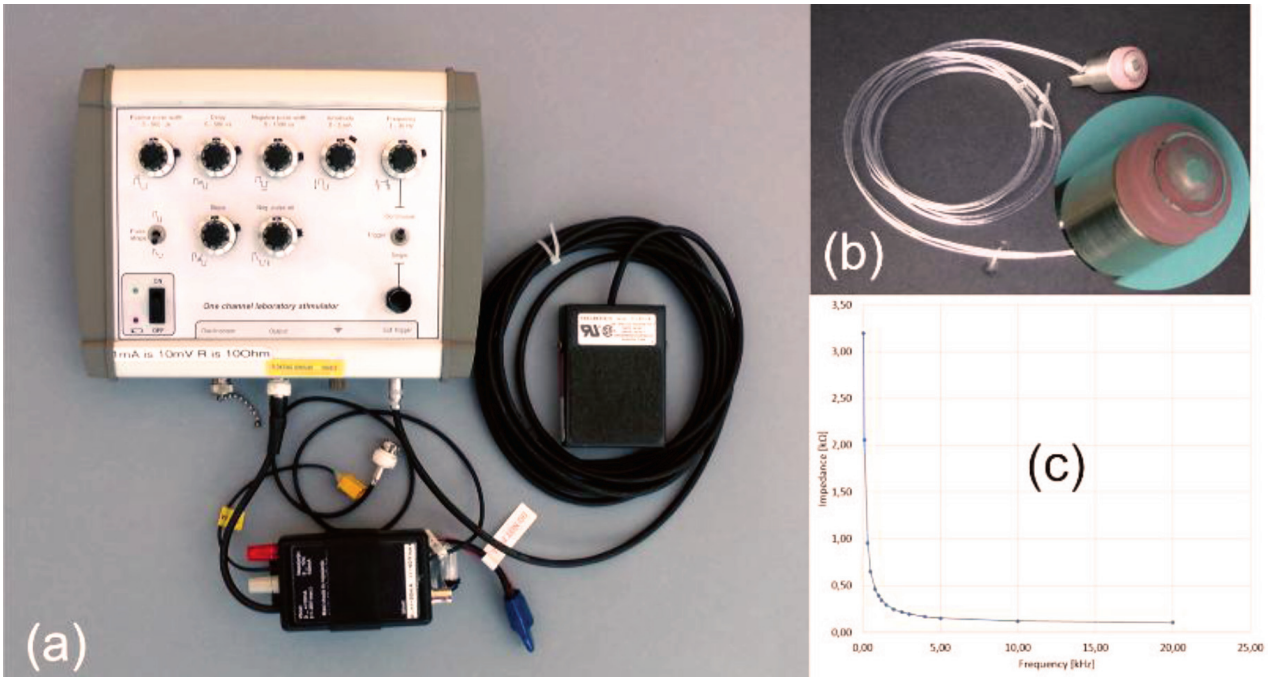

Figure 2: Stimulating setup: a) nerve stimulator with voltage booster amplifier and external trigger switch, b) probe with central stimulating cathode and ring-shape anode, c) impedance |Z| versus frequency

The performance of the stimulating set-up was investigated "in vitro" in phosphate-buffered saline solution. Corresponding impedance |Z| versus frequency is shown in **Figure 2**c.

For sterilization of the probe, low tempeature (50 °C) hydrogen peroxide gas plasma sterilization was selected. It is estimated as a safe and efficient alternative for PMMA, for FEP and, for PO-X sterilization even after multiple sterilizations.[20]

2.2 Measuring devices and proceduress

To monitor and evaluate the erectile events during NVBS, the multisensorial probe shown in the **Figure 3** was developed.

To measure ARIG in penises of different sizes, three bell-shape probes were crafted. Appropriate size might be selected and mounted onto the adapted force transducer (Type S2, Hottinger Brüel & Kjær GmbH, Darmstadt, Germany) (**Figure 3a**).

To measure T_{gp}, IR thermometer (CJMCU-614 (Wuxi Sichiray Co., Ltd., China) and IR sensor was attached onto a particular bell-shape probe (**Figure 3b**).[21]

To monitor GSR, a GSR device (GSR BI GSR BIOFEEDBACK, Prasad Psycho Private Limited, Gautam Budh Nagar, India), was used. The GSR signal should be sensed with two electrodes (geometric surface 484 mm^2) shown in the **Figure 3c**. They were made of a copper-zinc alloy ribbon (CU 80.28 %, Zn 19,64 %) and adhered into the bell-shape probe.[22,23]

To capture toe photoplethysmogram (TPG), pulse oximeter (Nellcor N-600, Tyco Healthcare Group LP, Nellcor Puritan Bennett Division, Pleasanton, CA, U.S.A.) and customized sensor shown in the **Figure 3d** were used.

To measure the variations of ambient temperature, the negative temperature coefficient (NTC) temperature sensor (Model JP402, J. P. Sensor, Hefei, Anhui, China) shown in the **Figure 3e** was used.

To measure the CCM activity, a dual-channel CC-EMG amplifier (ETH-256 2-Channel Bridge/ECG/EMG/EEG/Bio-Amplifier) and isolated biopotential preamplifier (C-ISO-256, iWorx/CB Sciences, Dover, U. S. A.) were used. CC-EMG was measured combining two surface and two intracavernous needle electrodes attached between the base. Platinum-iridium disposable needle electrodes (TE/S46-638, Technomed Europe, Maastricht-Airport, The Netherlands) were connected to positive inputs of the preamplifier. They were inserted into the left CC at 3 and into the right CC at 9 o'clock positions, as shown in the **Figure 4**. Their tips were positioned around the centre of the left and right CC.

Disposable surface silver/silver chloride electrodes (Part Number 019-400400, Natus, Middleton, USA) were connected to negative inputs of the preamplifier and placed onto the penile shaft as close as possible to

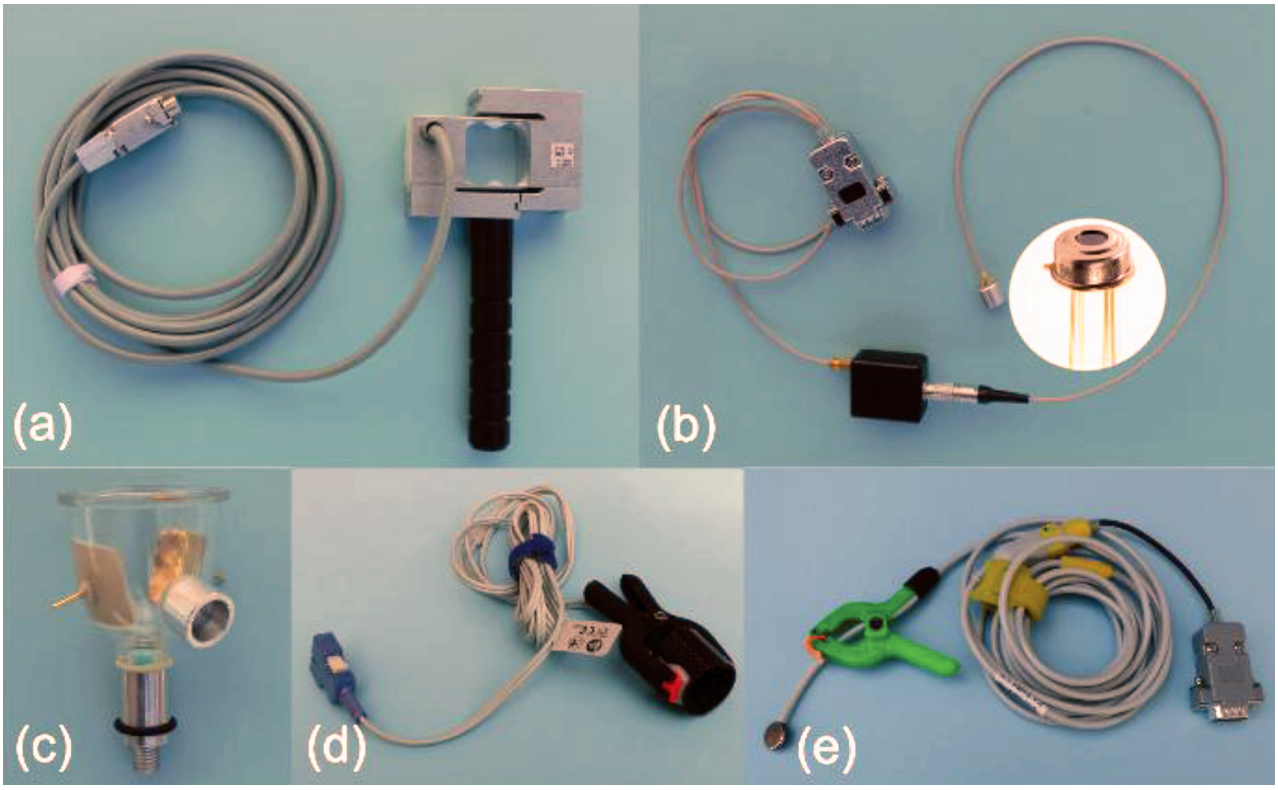

Figure 3: Multisensorial probe: a) force transducer, b) IR thermometer and IR chip sensor, c) electrodes for sensing GSR, d) TPG sensor, e) NTC sensor of ambient temperature

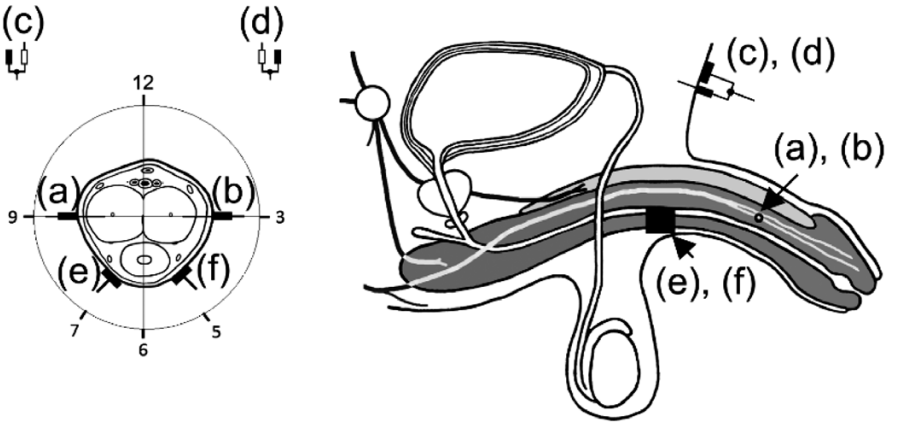

Figure 4: Positioning of CC-EMG electrodes on the penile shaft: a) right subdermal needle electrode, b) left subdermal needle electrode, c) right pubis reference electrodes, d) left pubis reference electrodes, e) right surface CC-EMG electrode, f) left surface CC-EMG electrode

Table 1: Parameters of rectangular and quasitrapezoidal stimuli

Parameter	Acronym	Rectangular pulses	Quasitrapezoidal pulses
Intensity of cathodic phase	i_c	variable between 10 and 30 mA	variable between 10 and 30 mA
Width of cathodic phase	t_c	160 µs	160 µs
Delay between phases	d	80 µs	NA
Width of exponential cathodic phase	t_{exp}	NA	80 µs
Time constant of exponential cathodic phase	τ_{exp}	NA	arbitrary set µs
Intensity of anodic phase	i_a	10-30 mA	10 mA
Width of anodic phase	t_a	160 µs	160 µs
Frequency	f	10 Hz	10 Hz
Stimulating/cathodic charge	Q_c	0.228–0.685 µC/mm^2	<0.228 – <0,685 µC/mm^2

the penis base. They were placed onto the left CC at 5 and onto the right CC at 7 o'clock positions as shown in the **Figure 4**.

Finally, combination of surface and needle ground electrodes was placed on the left and right pubis, respectively.[24]

2.3 Experimental Procedures

General anesthesia was induced with intravenous propofol (Diprivan) (Propofol 1% Fresenius, Fresenius Kabi, Germany). Afterwards, remifentanil hydrochloride (Ultiva, GlaxoSmithKline Export, Brentford, UK) was given as an analgesic and vecuronium bromide (Norcuron, Organon Laboratories, Cambridge, UK) was administered intravenously as a muscle relaxant.[25] Paracetamol is used to treat pain and fever (high temperature), Dexamethasone is used to provide relief for inflamed areas of the body, Pantoprazole (Protonix) is used to avoid conditions that cause too much stomach acid and Co-amoxiclav is used to avoid bacterial urinary tract infection. General anesthesia during prostatectomy took about two hours.

The probe was imported into the operating space via the fifth lateral 12-mm port (AirSeal®). The probe was guided by applying a firm grip on the titanium ayelet at the probe using a laparoscopic grasper of the daVinci Xi surgical system (Intuitive, Sunnyvale, California, U.S.A.). Stimuli were delivered to the NVB via lead wires placed within the port and electrodes at the probe (**Figure 2**) prior and after prostatic removal. To assess the integrity of the NVBs, the probe was placed for around 60 seconds on top, on middle and on base once of the left and once on the right NVB, respectively.

Table 1 depicts parameters of rectangular[26] and quasitrapezoidal pulses.[27]

To reduce DC offset, parameters were set such that Q_c and Q_a injected were nearly equal. During NVBS, intensity i_c started at 0 mA and increased to a maximum of 30 mA.

After sparing, the probe was pressed gently onto the NVB[28] so the thin flattened structues of the NVB were bent slightly into a basin surrounding the probe (**Figure 1**). Placement of the probe with robotic arm was done with particular care avoiding any stretch of the NVB.

To assess ARIG, GSR and T_{gp}, the experimenter would only push the bell-shaped probe axially onto the glans. If no ARIG rise was observed, the contralateral NVB was assessed. If no ARIG rise was observed again, an assessment was abandoned. Instead, only concomitant assessment of the right CC-EMG (CC-EMG$_r$) and left CC-EMG (CC-EMG$_l$) as well as TPG was accomplished. The raw CC-EMG signals were amplified (A = 40,000) and filtered (low-pass filter at 5 Hz, high-pass filter at 0.03 Hz).

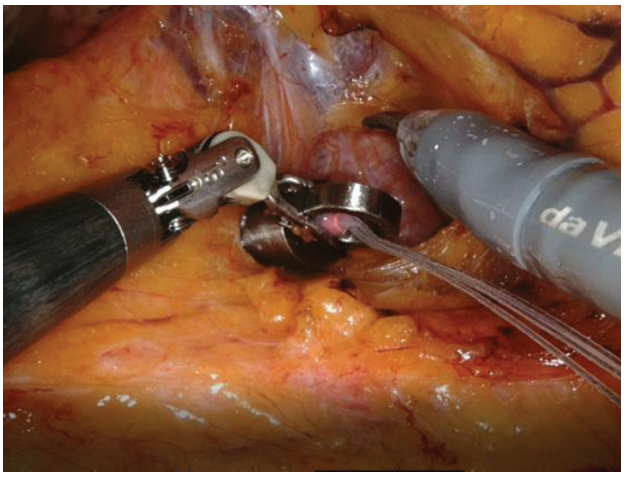

Figure 5: Probe placed on the right NVB

All the measured and conditioned signals were gathered at 20 kHz with 24-bit resolution using an acquisition systems (DEWE-43A, DEWESOFT d.o.o., Trbovlje, Slovenia). Finally, data were stored on a hard drive for off-line analysis using a software (DEWESoft 7.0.2) from the same company. During both NVBS assessments, ARIG, CC-EMG, glans temperature and GSR variations should be measured and recorded for off-line analysis.[29]

Since only preliminary results were obtained, no statistical comparisons could be made as part of this study.

3 RESULTS

Figure 6 represents results of NVBS at different sites and different intensity i_c in one of 5 patients enroled. Precisely, **Figure 6** only represents CC-EMG$_r$, CC-EMG$_l$ and TPG while different sites of the left and right NVB were stimulated. Term L identifies left NVB, term R identifies right NVB, term U identifies upper part of the NVB and L identifies lower part of the NVB. Traces in **Figure 6a** show: top-i_c, one below-CC-EMG$_r$, two below-CC-EMG$_l$ and bottom-TPG during NVBS of upper part of the left NVB before RARP (1UL). Traces in **Figure 6b** show: top-i_c, one below-CC-EMG$_r$, two below-CC-EMG$_l$ and bottom, TPG during NVBS of upper part of the left NVB after RARP (2UL). Traces in **Figure 6c** show: top-i_c, one below-CC-EMG$_r$, two be-

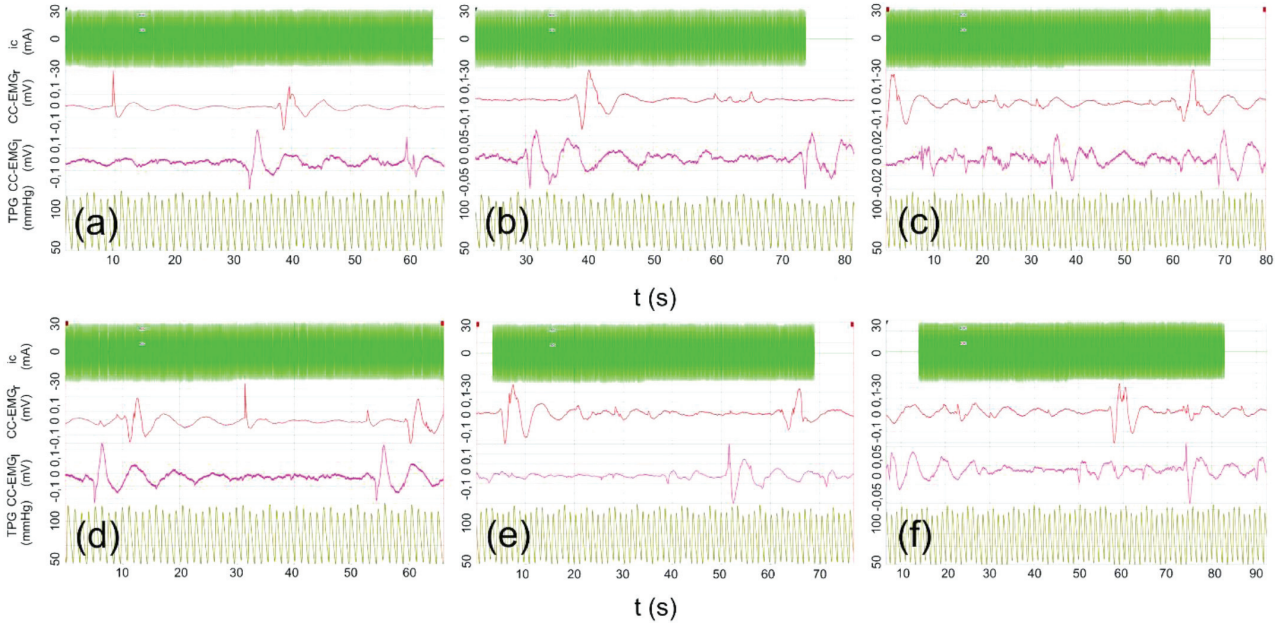

Figure 6: CC-EMG$_r$ and CC-EMG$_l$ while different sites of left and right NVB were stimulated. Details a to f show: top trace i_c, trace one below CC-EMG$_r$, trace two below CC-EMG$_l$ and bottom trace TPG. Stimulated NVB sites: a) 1UL, b) 2UL, c) 2LL, d) 1UR, e) 2UR and f) 2LR

Table 2: Measured quantities

Ch	Quantity	Acronym	Unit	Filter
1	Stimulating current	i_c	mA	off
2	Penile axial rigidity	ARIG	mN	Bessel, Low Pass 10 Hz, 2nd
3	Right Corpus Cavernosum EMG	CC-EMG$_r$	mV	4 pole active, Low Pass 5 Hz, High Pass 0.03 Hz
4	Left Corpus Cavernosum EMG	CC-EMG$_l$	mV	4 pole active, Low Pass 5 Hz, High Pass 0.03 Hz
5	Glans penis temperature	T_{gp}	°C	Bessel, Low Pass 10 Hz, 2nd
6	Galvanic skin response	GSR	kΩ	Bessel, Low Pass 10 Hz, 2nd
7	Toe photoplethysmogram	TPG	mmHg	Antialiasing filter (IIR)

Table 3: Quantities measured during selective NVBS

Stimulating Conditions				Measured Quantities						
Stimu-lated NVB	Pulse Type	i_c [mA]	Length [s]	CC-EMG I amplitude [μVpp]	CC-EMG II amplitude [μVpp]	IIEF before RARP	IIEF 3 months after RARP	Length CC-EMG I [s]	Length CC-EMG II [s]	Time delay between CC-EMG peaks [s]
1UL	Rectangular	25±5	60	NA	NA	12	9	NA	NA	NA
	Quasitrapezoidal	25±5	60	379,61	263,62			4,37	4,2	49,4
2UL	Rectangular	25±5	60	306,22	83,5			NA	4,56	NA
	Quasitrapezoidal	25±5	60	NA	84,23			5,12	4,7	42,89
2LL	Rectangular	25±5	60	274,39	85,47			NA	NA	62
	Quasitrapezoidal	25±5	60	252,71	90,97			5,9	4,6	34,7
1UR	Rectangular	25±5	60	281	232			3,6	4,28	49,16
	Quasitrapezoidal	25±5	60	289	220,5			5	3,97	49,36
2UR	Rectangular	25±5	60	298,5	NA			5,05	NA	58,43
	Quasitrapezoidal	25±5	60	211,84	302			5,9	5,72	NA
2LR	Rectangular	25±5	60	NA	100			NA	NA	53,47
	Quasitrapezoidal	25±5	60	265,44	160			5	6,6	66
Average				284,3	162,23	12	9	5	4,83	51,71

low-CC-EMG$_l$ and bottom-TPG during NVBS of lower part of the left NVB after RARP (2LL). Traces in **Figure 6d** show: top-i_c, one below-CC-EMG$_r$, two below-CC-EMG$_l$ and bottom-TPG during NVBS of upper part of right NVB before RARP (1UR). Traces in **Figure 6e** show: top-i_c, one below-CC-EMG$_r$, two below-CC-EMG$_l$ and bottom-TPG during NVBS of upper part of right NVB after RARP (2UR). Traces in **Figure 6f** show: top-i_c, one below-CC-EMG$_r$, two below-CC-EMG$_l$ and bottom-TPG during NVBS of lower part of right NVB after RARP (2LR).

Table 3 depicts the quantities measured in one of the patients during NVBS using 60-second trains of different types of stimuli. These quantities are the following: Stimulating current i_c, voltage peak of CC-EMG$_r$, voltage peak of CC-EMG$_l$, IIEF before RARP, IIEF 3 months after RARP, length of the first/largest sine of CC-EMG$_r$, length of the first/largest sine of CC-EMG$_l$ and time delay/latency between peaks of CC-EMG signals. Terms in **Table 3** identify: L-left NVB, R-right NVB, U-upper part of the NVB and L-lower part of the NVB.

4 DISCUSSION

RARP is considered as the standard treatment for prostate cancer with relatively good long-term results. However, surgeons still do not have common guidelines on this subject.[30] To optimize oncological and functional outcomes of the RARP, various nerve-sparing techniques have been developed.[31] This study describes the design, development, and feasibility testing of a system for selective NVBS during RARP. The aim was to induce an erection and to discuss the possibility of applying this system to predict EF after the RARP.

For this purpose, stimulating setup was developed to help to determine whether the NVBs have been successfully preserved after RARP. With regard the testing, the paradigm of fiber-type selective NVBS using two types of stimuli proposed testing during, before and after NVB sparing. An aim was to identify differences in EF that could be obtained using NVBS.

To explore the utility of NVBS during RARP and to assess which NVBS conditions made the most probable contribution to the erection, we constructed especial multisensorial probe.[26,28] It comprised sensor of ARIG, electrodes for sensing GSR and sensor of *T*gp.[32] The usefulness of the multisensorial probe developed should be assessed simply by placing it onto the penis during the NVBS. To reflect potential erectile events, the T_{PG} was measured expecting that in erection, arterial blood inflow and SpO_2 are increased. In **Figure 6**, CC-EMG waveforms measured at left and right CC during NVBS of different sites at the left and right NVB, are represented. It may be seen that peak-to-peak amplitudes of CC-EMG$_r$ and CC-EMG$_l$ are different. However, due to the small number of CC-EMG waves, a cause for generation of theese differences could not be identified. In **Figure 6a** and **Figure 6f**, artefacts between CC-EMG waves were seen. They appeared after switching between two types of stimuli. It is shown in **Table 3** that the average peak-to-peak amplitude of 284.3 μV in CC-EMG$_r$, is almost as twice as average peak-to-peak amplitude of 162.23 μV in CC-EMG$_l$. It might be seen that both CC-EMGs had gently sloping path, presumably as a result of a sharp filtering within a band between 0,05 and 5 Hz. It is also shown that 5 s long average length of CC-EMG$_r$ is only slightly larger than 4.83 s long average length of CC-EMG$_l$. Finally, it is seen that time delay between CC-EMG peaks was 51,71 s. The most important quantity that describes EF after RARP, namely IIE=9, was about 25 % lower than IIEF=1 before RARP.

The main strengths of the system are the following:

– Potential adverse events and risks related to NVBS were low relative to those of RARP.

– An i_c used in NVBS have been proven safe.
– Cathodic charge (Q_c) used with both types of stimuli was accptable for short term NVBS.
– No adverse events with intercavernosal CC-EMG needle electrode insertion, were observed.
– No adverse events related to probe manipulated by principal investigator/urologist, were noticed.
– Currently there does not exist NVBS paradigm that combines spatial and fibre-type stimulation of CN and NVBs.

The main weakness of testing the system were short time periods dedicated for NVBS during regular RARP procedures. Namely, 60 s long recordings were too short to provide an adequate interpretation of results and an efficiency of NVBS. Since time delay/latency between peaks of CC-EMG waves was around 60 s, these recordings could comprise only two CC-EMG waves.

Beside this, NVBS have not resulted in measurable erections, so multisensorial probe failed to provide any signal and overall EF have not been assessed. Possible reasons for lack of erection:

– Before sparing, NVB branches were dispersed bilaterally on the prostate so stimulating cathode established electrical contact with relatively small number of NVB branches. Accordingly, neural drive to the CC was relatively weak.
– After sparing, NVB branches were dispersed bilaterally within both separated tissues so stimulating cathode established electrical contact with relatively small number of NVB branches. Accordingly, neural drive to the CC was relatively weak.
– In some patients, cancerous tissue was spread between NVB branches so i_c density was too low to depolarize larger number of NVB branches.
– In some patients, fat tissue was spread between NVB branches so i_c density was too low to depolarize a larger number of NVB branches.

Thus, short recordings could not be analysed in the frequency or time domain, but they could reflect a short-term monitoring of CC-EMG during the RARP. In any case, CC-EMG monitoring during RARP provided some important information on the status of the NVB tissue after RARP in patients with pre-operatively intact EF.[33] In order to obtain a more consistent picture on the status of the NVB tissue just after RARP, further research should consider prolonging the NVBS during RARP. Beside this, in order to elicit increase in ARIG during RARP, further improvement in NVBS scheme should be implemented. With this regard, a probe with larger and modified area of stimulating electrodes will be crafted. Multisensorial probe developed could be used in urological practice for identification of relation between the CC pressure and penile ARIG and in evaluation of new vasoactive agents on erection.

5 CONCLUSIONS

This preliminary report provides an evidence that probe can effectively deliver electrical stimuli to the penis while placed onto the NVB during RARP. Among 5 men enrolled in this study, 2 (40 %) demonstrated noticable incidence of CC-EMG waves, but none of them demonstrated a measurable increase in penile axial rigidity in response to NVBS. A multisensorial probe developed was a useful tool with respect to research, prevention, diagnosis and treatment of ED. Although the applied stimulation protocol did not induce measurable erectile responses, CC-EMG signals provided potentially valuable intraoperative insights into NVB integrity. With this information, it may be easier to predict the status of erectile function after the RARP. The results obtained may be potentially useful in further development of chronic implantable devices to be used for recovery of EF following RARP.

Acknowledgment

This work was financed by the research grant P3-0171 from the Slovenian Research and Innovation Agency (ARIS), Ministry of Education, Science and Sport, Ljubljana, Republic of Slovenia.

6 REFERENCES

[1] UFHealth. Robotic Nerve-Sparing Radical Prostatectomy https://urology.ufl.edu/patient-care/robotic-laparoscopic-urologic-surgery/procedures/robotic-nerve-sparing-radical-prostatectomy/

[2] P. C. Walsh, H. Lepor & J. C. Eggleston, Radical prostatectomy with preservation of sexual function: Anatomical and pathological considerations, The Prostate, 4(**1983**)5, 473–485, doi:10.1002/pros.2990040506

[3] H. Lepor, M. Gregerman, R. Crosby, F. K. Mostofi & P. C. Walsh, Precise localization of the autonomic nerves from the pelvic plexus to the corpora cavernosa: a detailed anatomical study of the adult male pelvis, J. Urol., 133(**1985**)2, 207–212, doi:10.1016/s0022-5347(17)48885-9

[4] P. N. Schlegel, P. C. Walsh, Neuroanatomical approach to radical cystoprostatectomy with preservation of sexual function, J. Urol., 138(**1987**)6, 1402–1406, doi:10.1016/s0022-5347(17)43655-x

[5] P. C. Walsh, J. I. Epstein & F. C. Lowe, Potency following radical prostatectomy with wide unilateral excision of the neurovascular bundle J. Urol., 138(**1987**)4, 823–827, doi:10.1016/s0022-5347(17)43385-4

[6] J. Rehman, G. J. Christ, A. Kaynan, D. Samadi & J. Fleischmann, Intraoperative electrical stimulation of cavernosal nerves with monitoring of intracorporeal pressure in patients undergoing nerve sparing radical prostatectomy, BJU Int., 84(**1999**)3, 305–310, doi:10.1046/j.1464-410x.1999.00143.x

[7] A. J. Costello, M. Brooks & O. J. Cole, Anatomical studies of the neurovascular bundle and cavernosal nerves, BJU Int. 94(**2004**)7, 1071–1076, doi:10.1111/j.1464-410X.2004.05106.x

[8] S. Yucel, T. Erdogru, M. Baykara, Recent neuroanatomical studies on the neurovascular bundle of the prostate and cavernosal nerves: clinical reflections on radical prostatectomy, Asian Journal of Andrology, 7(**2005**)4, 339–349, doi:10.1111/j.1745-7262.2005.00097.x

[9] S. Hisasue, K. Hashimoto, K. Kobayashi, M. Takeuchi, Y. Kyoda, S. Sato, N. Masumori & T. Tsukamoto, Baseline erectile function alters the cavernous nerve quantity and distribution around the prostate, J. Urol., 184(**2010**)5, 2062–2067, doi:10.1016/j.juro.2010.06.108

[10] J. Walz, A. L. Burnett, A. J. Costello, J. A. Eastham, M. Graefen, B. Guillonneau, M. Menon, F. Montorsi, R. P. Myers, B. Rocco & A. Villers, A critical analysis of the current knowledge of surgical anatomy related to optimization of cancer control and preservation of continence and erection in candidates for radical prostatectomy, Eur. Urol., 57(**2010**)2, 179–92, doi:10.1016/j.eururo.2009.11.009

[11] B. Alsaid, I. Karam, T. Bessede, I. Abdlsamad, J.-F. Uhl, V. Delmas, G. Benoît & S. Droupy, Tridimensional Computer-Assisted Anatomic Dissection of Posterolateral Prostatic Neurovascular Bundles, Eur. Urol., 58(**2010**)2, 281–287, doi:10.1016/j.eururo.2010.04.002

[12] B. Alsaid, T. Bessede, D. Diallo, D. Moszkowicz, I. Karam, G. Benoît & S. Droupy, Division of autonomic nerves within the neurovascular bundles distally into corpora cavernosa and corpus spongiosum components: immunohistochemical confirmation with three-dimensional reconstruction, Eur. Urol., 59(**2011**)6, 902–909, doi:10.1016/j.eururo.2011.02.031

[13] G. M. Villeirs, K. L.Verstraete, W. J. De Neve & G. O. De Meerleer, Magnetic Resonance Imaging Anatomy of the Prostate and Periprostatic Area: A Guide for Radiotherapists, Radiother. Oncol., 76(**2005**)1, 99-106, doi:10.1016/j.radonc.2005.06.015

[14] E. E. Clarebrough, B. J. Challacombe, C. Briggs, B. Namdarian, R. Weston, D. G. Murphy & A. J. Costello, Cadaveric Analysis of Periprostatic Nerve Distribution: An Anatomical Basis for High Anterior Release During Radical Prostatectomy? J. Urol., 185(**2011**)4, 1519–1525, doi:10.1016/j.juro.2010.11.046

[15] H. W. Axelson, E. Johansson & A. Bill-Axelson, Intraoperative Cavernous Nerve Stimulation and Laser-Doppler Flowmetry during Radical Prostatectomy, J. Sex. Med., 10(**2013**)11, 2842–2848, doi:10.1111/j.1743-6109.2012.02892.x

[16] G. Y. Tan, S. Grover, A. Takenaka, P. Sooriakumaran, A. K. Tewari, Current Concepts in Cavernosal Neural Anatomy and Imaging and Their Implications for Nerve-Sparing Radical Prostatectomy in Robotics in Genitourinary Surgery, Springer, London 2011, 273–289, doi:10.1007/978-1-84882-114-9_24

[17] S. Unal, B. Musicki & A. L. Burnett, Cavernous nerve mapping methods for radical prostatectomy, Sex. Med. Rev., 11(**2023**)4, 421–430, doi:10.1093/sxmrev/qead030

[18] Z.-P. Fang, J. T. Mortimer, Selective activation of small motor axons by quasitrapezoidal current pulses, IEEE Trans. Biomed. Eng., 38(**1991**)2, 168–174, doi:10.1109/10.76383

[19] E. M. Hudak, J. T. Mortimer & H. B. Martin, Platinum for neural stimulation: voltammetry considerations, J. Neural Eng., 7(**2010**)2, 26005, doi:10.1088/1741-2560/7/2/026005

[20] T. J. A. G. Münker, S. E. C. M. van de Vijfeijken, C. S. Mulder, V. Vespasiano, A. G. Becking, C. J. Kleverlaan, A. G. Becking, L. Dubois, L. H. E. Karssemakers, D. M. J. Milstein, S. E. C. M. van de Vijfeijken, P. R. A. M. Depauw, F. W. A. Hoefnagels, W. P. Vandertop, C. J. Kleverlaan, T. J. A. G. Münker, T. J. J. Maal, E. Nout, M. Riool & S. A. J. Zaat, Effects of sterilization on the mechanical properties of poly(methyl methacrylate) based personalized medical devices, J. Mech. Behav. Biomed. Mater., 81(**2018**), 168–172, doi:10.1016/j.jmbbm.2018.01.033

[21] S. Asadian, A. Khatony, G. R. Moradi, A. Abdi, & M. Rezaei, Accuracy and precision of four common peripheral temperature measurement methods in intensive care patients, Med. Devices (Auckl.), 9(**2016**), 301–308, doi:10.2147/MDER.S109904

[22] V. F. S. Tsai, H.-C. Chang, S.-P. Liu, Y.-C. Kuo, J.-H. Chen, F.-S. Jaw & J.-T. Hsieh, Determination of Human Penile Electrical Resistance and Implication on Safety for Electrosurgery of Penis, J. Sex. Med., 7(**2010**)8, 2891–2898, doi:10.1111/j.1743-6109.2010.01856.x

[23] A. Sanchez-Comas, K. Synnes, D. Molina-Estren, A. Troncoso-Palacio & Z. Comas-González, Correlation Analysis of Different Measurement Places of Galvanic Skin Response in Test Groups Facing Pleasant and Unpleasant Stimulating pulses, Sensors (Basel), 21(**2021**)12, 4210, doi:10.3390/s21124210

[24] S. E. Hyun, K. Kim, Intra-operative cavernous nerve monitoring and mapping during radical prostatectomy: a case report of corpus cavernosum electromyography, J. Intraoper. Neurophysiol., 3(**2021**)2, 97–101, doi:10.33523/join.2021.3.2.97

[25] G. U. Roh, Y. Song, J. Park, Y. M. Ki & D. W. Han, Effects of propofol on the inflammatory response during robot-assisted laparoscopic radical prostatectomy: a prospective randomized controlled study, Sci. Rep., 9(**2019**), 5242, doi:10.1038/s41598-019-41708-x

[26] A. Takenaka, A. Tewari, R. Hara, R. A. Leung, K. Kurokawa, G. Murakami & M. Fujisawa, Pelvic autonomic nerve mapping around the prostate by intraoperative electrical stimulation with simultaneous measurement of intracavernous and intraurethral pressure, J. Urol., 177(**2007**)1, 225–229, doi:10.1016/j.juro.2006.08.104

[27] P. Pečlin & J. Rozman, Alternative paradigm of selective vagus nerve stimulation tested on an isolated porcine vagus nerve, The Scientific World Journal 2014(**2014**), 310283, doi:10.1155/2014/310283

[28] A. L. Burnett & T. F. Lue, Neuromodulatory therapy to improve erectile function recovery outcomes after pelvic surgery, J. Urol., 176(**2006**)3, 882–7, doi:10.1016/j.juro.2006.04.020

[29] W. H. Song, J. H. Park, B. S. Tae, S.-M. Kim, M. Hur, J.-H. Seo, J. H. Ku, C. Kwak, H. H. Kim, K. Kim & C. W. Jeong, Establishment of novel intraoperative monitoring and mapping method for the cavernous nerve during robot-assisted radical prostatectomy: results of the phase I/II, first-in-human, feasibility study, Eur. Urol., 78(**2020**)2, 221–228, doi:10.1016/j.eururo.2019.04.042

[30] R. Tal, P. Teloken & J. P. Mulhall, Erectile function rehabilitation after radical prostatectomy: Practice patterns among AUA members, J. Sex. Med., 8(**2011**)8, 2370–2376, doi:10.1111/j.1743-6109.2011.02355.x

[31] I. Kyriazis, T. Spinos, A. Tsaturyan, P. Kallidonis, J. U. Stolzenburg & E. Liatsikos, Different Nerve-Sparing Techniques during Radical Prostatectomy and Their Impact on Functional Outcomes. Cancers (Basel) 14(**2022**)7, 1601, doi:10.3390/cancers14071601, doi:10.3390/cancers14071601

[32] I. Goldstein, D. G. Udelson, Axial penile rigidity: determinants and relation to hemodynamic parameters, Int. J. Impot. Res., 10(**1998**)2, S28–33, discussion S49-51

[33] G. Wagner, X. Jiang, Corpus cavernosum electromyography, a usable clinical diagnostic method for erectile dysfunction? Indian Journal of Urology, 22(**2006**)3, 225–230, doi:10.4103/0970-1591.27629